JOURNAL OF SOLID STATE CHEMISTRY 80, 195–200 (1989)

High-Resolution Solid-State ^{31}P NMR Study of Network Structure in $AgI–Ag_2O–P_2O_5$ Glass

SHIGENOBU HAYASHI* AND KIKUKO HAYAMIZU

National Chemical Laboratory for Industry, Tsukuba, Ibaraki 305, Japan

Received December 5, 1988; in revised form February 27, 1989

High-resolution solid-state ^{31}P NMR spectra have been measured for $AgI–Ag_2O–P_2O_5$ glasses using magic-angle sample spinning. Three types of PO_4 units can be identified: isolated, end chain, and middle chain groups. Quantitative analysis has been carried out for the three groups, and the average length of the PO_3 chain has been estimated. The NMR results have confirmed that the network structure is determined by the two components, Ag_2O and P_2O_5, and that AgI does not modify the network.

Introduction

Vitreous ionic conductors have attracted much interest in recent years (*1, 2*). Glasses have advantages over crystalline electrolytes in the following aspects: (a) Glasses are physically isotropic, and have no grain boundaries, (b) the composition can be varied continuously, and (c) their processing is relatively easy. Furthermore, conductivity higher than that of crystals has been reported for some systems (*3–5*). Among the vitreous ionic conductors, $AgI–Ag_2O–P_2O_5$ system has one of the highest ionic conductivities. The system has the maximum ionic conductivity of the order of 10^{-2} S cm^{-1} at 25°C (*3, 6*), which is comparable with aqueous solutions of electrolytes.

Several structural models have been proposed to explain such high conductivity in vitreous electrolytes. One model is that clusters or microdomains of silver halides are embedded in the host glass matrix; it is termed the cluster model (*7, 8*). Another model is that silver halide is dispersed into the glass network (*9, 10*). Which model is better to explain the glass structure has not yet been established.

The structure of the $AgI–Ag_2O–P_2O_5$ glass has been studied by means of several methods: Raman scattering (*7*), quasielastic neutron scattering (*11*), infrared spectroscopy (*12*), thin-layer chromatography (*12*), X-ray diffraction (*13*), and so on.

High-resolution solid-state NMR is a powerful tool to study the short-range order, and it is a nondestructive method (*14*). ^{31}P NMR can be expected to clarify the network structure composed of the PO_4 units (*15–20*). In the present work, we measured high-resolution solid-state ^{31}P NMR spectra and have elucidated the bonding structure of the glass network.

Experimental

Materials

Glasses were prepared using the procedure described by Minami *et al.* (*3*). The starting materials were purchased from

---

*To whom correspondence should be addressed.

0022-4596/89 $3.00

commercial sources: AgI and Ag_2O from Nakarai Chemicals Co., Ltd. (Kyoto, Japan), H_3PO_4 from E. Merck (Darmstadt), and Ag_3PO_4 and $Ag_4P_2O_7$ from Soekawa Chemicals Co., Ltd. (Tokyo, Japan). After heating the mixture of raw materials in a Pyrex glass ampoule at 500°C for 21 hr, the melt was poured onto a stainless-steel plate.

The compositions determined from the weight of the starting materials are listed in Table I and schematically shown in Fig. 1. The starting materials are different between the groups, as noted in Table I.

The crystallinity was checked by X-ray diffraction using a Rigaku Geiger-Flex diffractometer with Cu*Kα* irradiation. A Rigaku 8230 thermal analyzer was used to determine the glass transition temperature, T_g. The sample temperature was increased at a rate of 5 K/min in air. The crystallinity and the observed T_g values are listed in Table I. The glass-forming region and T_g obtained in the present work agree with the literature values (*3*).

TABLE I

COMPOSITION, GLASS TRANSITION TEMPERATURE, AND CRYSTALLINITY OF THE GLASSES

Group No.[a]	Sample No.	Composition (mole%) AgI	Ag_2O	P_2O_5	T_g (°C)	χ_c[b]
I	1	69.7	20.2	10.1	Unclear	gc
	2	64.8	23.5	11.7	46	g
	3	60.0	26.7	13.3	58	g
	4	54.9	30.1	15.0	62	g
	5	49.8	33.4	16.7	65	g
	6	45.1	36.6	18.3	68	g
II	7	70.0	22.5	7.5	Unclear	gc
	8	65.3	26.0	8.7	54	gc
	9	60.0	30.0	10.0	61	gc
	10	55.0	33.8	11.3	65	gc
III	11	69.7	25.4	4.9	None	cr
	12	64.9	25.1	10.0	Unclear	gc
	13	60.0	25.0	15.0	55, 60[c]	g
	14	54.9	25.1	20.0	61, 70[c]	g
	15	49.8	25.3	24.9	64, 87[c]	g
	16	45.0	25.1	29.8	68, 87[c]	gs
	17	42.1	21.3	36.5	Unclear	gc

[a] Group I was prepared from AgI and $Ag_4P_2O_7$, Group II from AgI and Ag_3PO_4, and Group III from AgI, Ag_2O, and H_3PO_4.

[b] g, glass; gs, glass with a small amount of crystal (less than 10%); gc, mixture of glass and crystal; cr, crystal.

[c] The second endothermic peak was observed.

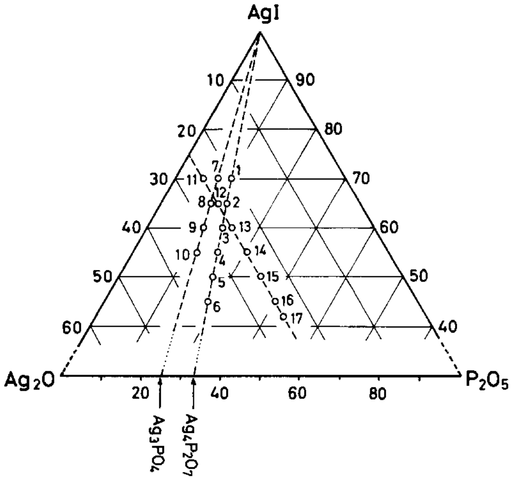

FIG. 1. Composition of the glasses, expressed in mole%.

NMR Measurements

High-resolution solid-state ^{31}P NMR spectra were measured using a JEOL FX-200 pulsed spectrometer equipped with accessories for magic-angle sample spinning (MAS) (*21, 22*) at the resonance frequency of 80.76 MHz and at an ambient temperature. The ordinary single-pulse sequence was used, in which a flip angle of the pulse was set at $\pi/4$ and the recycle time was 15 sec. The samples were pulverized into fine powder, and then they were packed into a rotor made of Delrin. The rotor was spun at about 3.5 kHz. The shift value is given with respect to 85% H_3PO_4 aqueous solution, with the higher frequency being positive.

Results and Discussion

^{31}P NMR Spectra

Figure 2 shows ^{31}P MAS NMR spectra of two samples, No. 4 and No. 13. The isotropic peaks can be identified by changing

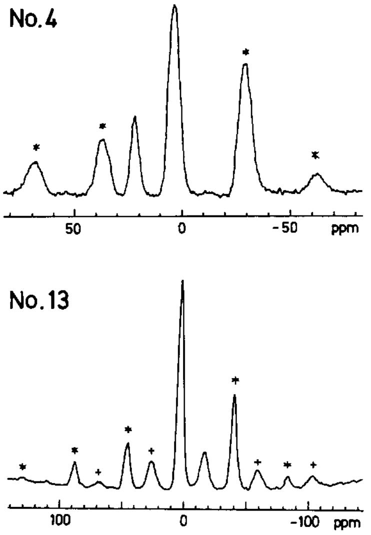

FIG. 2. ^{31}P MAS NMR spectra of the No. 4 and No. 13 samples. Signals marked with * are spinning sidebands of the 3-ppm line, while those marked with + are of the −15-ppm line.

the spinning rate of the sample. In the No. 4 sample, two sets of peaks were observed. Their isotropic chemical shifts are 21.8 and 3.1 ppm. In the No. 13 sample also, two sets of peaks were observed with their isotropic chemical shifts of 2.9 and −15.2 ppm. Many spinning sidebands are observed on both sides of the isotropic peaks due to the large chemical shift anisotropy in the ^{31}P nuclei. Similar spectra were obtained for other samples. Table II summarizes the isotropic chemical shift and intensity of all the samples studied. As is shown in the table, the glass samples have three types of peaks, whose isotropic chemical shifts are 21–23, 2–4, and −15 − 22 ppm, respectively. The No. 10 sample has a small shoulder at 16 ppm, which is considered to be included in the first group. The peaks in the crystalline part can be easily recognized, since their linewidth is much narrower than that of the glassy part. The −52-ppm peak in the No. 17 sample is out of the ranges of the above three groups, though it arises from the crystalline part. In the case where more than two sets of peaks are observed, the relative intensities are estimated except when they are not severely overlapped. The relative intensity can be estimated from the peak areas including sidebands, the results of which are shown in the parentheses in Table II. These intensities are proportional to the number of P atoms.

To assign the observed lines to some structures, the ^{31}P NMR spectra have been measured for crystalline compounds such as Ag_3PO_4 and $Ag_4P_2O_7$. Ag_3PO_4 and $Ag_4P_2O_7$ have the isotropic chemical shifts of 28.4 and 6.5 ppm, respectively. The 28.4-ppm peak can be ascribed to the isolated PO_4 group (named Q_0), while the 6.5-ppm peak can be ascribed to the end group of PO_4 chain (Q_1). Although some fine structures were observed in the spectra, they are not important in the present work and will be discussed elsewhere. The sharing of one oxygen atom between two PO_4 units causes

TABLE II

SUMMARY OF THE ^{31}P NMR RESULTS

Group No.	Sample No.	Chemical Shift (ppm)		Fraction (%)	
		Q_0	Q_1	Q_2	Q_3
I	1	20.9 (13)	2.7 (87)		
	2	20.7 (11)	2.4 (89)		
	3	22.0 (9)	2.3 (91)		
	4	21.8 (11)	3.1 (89)		
	5	22.5 (9)	3.9 (91)		
	6	23.0 (9)	4.2 (91)		
II	7	21.4[a] 20.5			
	8	21.3[b]			
	9	21.8[b]			
	10	21.6[a] 22 16[c]			
III	11	28.7[a]	6.2[a]		
	12		2.8 (80)	−16.3 (20)	
	13		2.9 (74)	−15.2 (26)	
	14		2.4 (28)	−18.9 (72)	
	15		3 (4)	−19.6 (96)	
	16			−20.6	
	17		0.3[a] (1)	−21.8 (97)	−52[a] (2)

[a] Peaks in the crystalline part.

[b] Peaks in the glassy and crystalline parts are superposed.

[c] Small shoulder.

the lower frequency shift of about 20 ppm. The same trend was observed in other phosphates (*15, 16, 19*). By analogy with these phosphates, the middle group of the PO_4 chain (Q_2) in the glass can be expected to be observed at about -20 ppm.

Following the above discussion, the peaks observed in the glasses can be assigned as follows: The 21- to 23-ppm peaks to the isolated PO_4 group (Q_0), the 2- to 4-ppm peak to the end PO_4 group of the chain (Q_1), and the -15- to -22-ppm peak to the middle PO_4 group in the chain (Q_2).

The observed chemical shift of Q_2 is dependent on the composition, while the dependence is small in the Q_0 and Q_1 units. The chemical shift of Q_2 decreases as the P_2O_5 concentration increases.

Structure of the Glass

The PO_4 groups are connected with each other sharing the oxygen atom to form the network structure of the glass. Ag ions are assumed to move in the network.

In group I, the ratio of $[Ag_2O]/[P_2O_5]$ is 2. It can be assumed that the structure of the PO_4 group is $P_2O_7^{4-}$ ion ($Q_1 - Q_1$) from the composition. Experimentally, the Q_1 units are dominant, but Q_0 units are also present with a fraction of about 10%. A part of them comes from the starting material $Ag_4P_2O_7$, which contains about 4% of Q_0 units as impurity, being checked by ^{31}P NMR. The other part of the Q_0 units is formed in the course of glass formation.

In group II, the ratio of $[Ag_2O]/[P_2O_5]$ is 3. Only the Q_0 units should be present in this composition. Experimentally, only the Q_0 units are observed.

In group III, the ratio of $[Ag_2O]/[P_2O_5]$ is smaller than 2, except for the No. 11 and No. 12 samples. Chains of PO_4 groups are formed, whose average length can be predicted from the composition and can be determined experimentally from the present results of ^{31}P NMR. The average chain length can be expressed by the following equations, assuming that only linear chains are formed having the formula $[Q_1] - [Q_2]_{n-2} - [Q_1]$.

$$n(\text{Composition}) = 2/(R - 1) \quad (1 < R \leq 2) \qquad (1)$$

$$n(\text{NMR}) = 2/[Q_1] \quad ([Q_1] + [Q_2] = 1), \qquad (2)$$

where n is the average number of PO_4 units in a chain, R is the ratio of $[Ag_2O]/[P_2O_5]$, and $[Q_1]$ is the fraction of Q_1 determined from the ^{31}P NMR. Table III lists the estimated length. Good agreements are observed except for the No. 12 sample. The PO_4 units are condensed up to the limit that the composition allows. This means that the ratio of $[Ag_2O]/[P_2O_5]$ determines the average chain length and that AgI does not modify it. As for the No. 12 sample, the X-ray diffraction result demonstrates the precipitation of AgI crystalline phase. The precipitation of the crystal might cause the deviation, but the exact reason is ambiguous.

The dependence of the chemical shift in Q_2 on the composition can be related to the chain length. The chemical shift is plotted in Fig. 3 as a function of the average chain length determined by NMR. The Q_2 peak shifts toward the lower frequency with the increase in the chain length. This trend presumably arises from the fact that Q_2 species nearer to the Q_1 endgroup have different chemical shift from interior Q_2 species.

TABLE III

THE AVERAGE CHAIN LENGTH IN THE GROUP III GLASSES

Sample No.	From composition		From NMR	
	R	n	$[Q_1]$	n
12	2.51	1.3	0.80	2.5
13	1.67	3.0	0.74	2.7
14	1.26	7.7	0.28	7.1
15	1.02	50	0.04	50
16	0.84	—	0.00	∞
17	0.58	—	0.00	∞

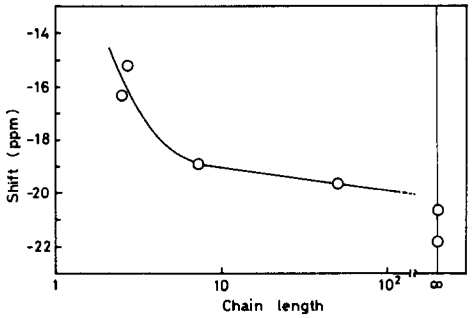

FIG. 3. The dependence of the chemical shift of Q_2 species on the average chain length estimated from ^{31}P NMR. The line in the figure is a guide to the eye.

Amorphousness convolutes the signals of various Q_2 species, since it produces chemical shift dispersion which cannot be eliminated by the MAS technique. The scatter of the observed values shown in Fig. 3 comes from the broad linewidth.

Equation (1) cannot be applied to the No. 16 and No. 17 samples, where $R < 1$. The composition demands the formation of branched chains. In the No. 17 sample an extra line was observed at −52 ppm, which can be ascribed to Q_3 locating at the branched position (*15, 16*), though it arises from the crystalline part.

Conclusively, the network structure is determined by the two components, Ag_2O and P_2O_5, and the third component, AgI, does not alter the network.

Minami *et al.* (*12*) have studied the structure of the present system by means of infrared spectroscopy (IR) and thin-layer chromatography (TLC). They concluded qualtitatively as follows: PO_4^{3-} ion (Q_0) is dominant for $R = 3$ and $P_2O_7^{4-}$ ion ($Q_1 - Q_1$) for $R = 2$, while linear chains of the PO_4 units are formed for $R < 2$. Malugani and Mercier (*7*) concluded from their Raman investigations that the skeleton of the PO_3 chains is not modified by the presence of Ag*X* (X = I, Br, and Cl). Musinu *et al.* (*13*) obtained similar results from an X-ray diffraction study. The present NMR results confirm the previous results quite straightforwardly.

The fact that the addition of a metal halide, *MX*, to a binary system is not associated with important modification of the network structure has been observed for other systems such as Ag*X*–Ag_2O–B_2O_3 (*23*) and Li*X*–Li_2O–P_2O_5 (*24*) (X = I, Br, and Cl) as well.

Roughly speaking, the ionic conductivity and T_g depend primarily on the AgI content (*3*). On the other hand, the PO_4 network structure depends mainly on the ratio of $[Ag_2O]/[P_2O_5]$. Thus the network structure is not the primary factor to determine the ionic conductivity and the glass transition temperature, but it can be the second factor. Supposing that the AgI content is constant, the ionic conductivity increases and the glass transition temperature decreases as R decreases (*3*). The above changes in the conductivity and the glass transition temperature might be correlated with the formation of the PO_4 chain.

References

1. T. MINAMI, *J. Non-Cryst. Solids* **73,** 273 (1985).
2. C. A. ANGELL, *Solid State Ionics* **18–19,** 72 (1986).
3. T. MINAMI, Y. TAKUMA, AND M. TANAKA, *J. Electrochem. Soc.* **124,** 1659 (1977).
4. T. MINAMI, H. NAMBU, AND M. TANAKA, *J. Amer. Ceram. Soc.* **60,** 283, 467 (1977).
5. T. MINAMI AND M. TANAKA, *J. Solid State Chem.* **32,** 51 (1980).
6. J. P. MALUGANI, A. WASNIEWSKI, M. DOREAU, AND G. ROBERT, *Mater. Res. Bull.* **13,** 427 (1978).
7. J. P. MALUGANI AND R. MERCIER, *Solid State Ionics* **13,** 293 (1984).
8. G. GARINI, M. CUTRONI, A. FONTANA, G. MARIOTTO, AND F. ROCCA, *Phys. Rev. B* **29,** 3567 (1984).
9. G. LICHERI, A. MUSINU, G. PASCHINA, G. PICCALUGA, G. PINNA, AND A. MAGISTRIS, *J. Chem. Phys.* **85,** 500 (1986).
10. A. MUSINU, G. PASCHINA, G. PICCALUGA, AND M. VILLA, *J. Chem. Phys.* **86,** 5141 (1987).
11. M. TACHEZ, R. MERCIER, J. P. MALUGANI, AND A. J. DIANOUX, *Solid State Ionics* **20,** 93 (1986).

12. T. Minami, T. Katsuda, and M. Tanaka, *J. Phys. Chem.* **83,** 1306 (1979).

13. A. Musinu, G. Piccaluga, and G. Pinna, *J. Chem. Phys.* **89,** 1074 (1988).

14. C. A. Fyfe, "Solid State NMR for Chemists," C.F.C., Guelph (1983).

15. A.-R. Grimmer and U. Haubenreisser, *Chem. Phys. Lett.* **99,** 487 (1983).

16. T. M. Duncan and D. C. Douglass, *Chem. Phys.* **87,** 339 (1984).

17. M. Villa, G. Chiodelli, and M. Scagliotti, *Solid State Ionics* **18–19,** 382 (1986).

18. G. L. Turner, K. A. Smith, R. J. Kirkpatrick, and E. Oldfield, *J. Magn. Reson.* **70,** 408 (1986).

19. S. Prabhakar, K. J. Rao, and C. N. R. Rao, *Chem Phys. Lett.* **139,** 96 (1987).

20. M. Villa, K. R. Carduner, and G. Chiodelli, *Phys. Chem. Glasses* **28,** 131 (1987).

21. E. R. Andrew, *Prog. Nucl. Magn. Reson. Spectrosc.* **8,** 1 (1972).

22. I. J. Lowe, *Phys. Rev. Lett.* **2,** 285 (1959).

23. D. P. Button, R. Tandon, C. King, M. H. Veléz, H. L. Tuller, and D. R. Uhlmann, *J. Non-Cryst. Solids* **49,** 129 (1982).

24. J. P. Malugani and G. Robert, *Mater. Res. Bull.* **14,** 1075 (1979).